Nonlinear Aerodynamic Predictions Of Aircraft and Missiles Employing Trailing-Edge Flaps

Daniel J. Lesieutre[1]
Nielsen Engineering & Research, Inc., Santa Clara, CA, 95054

The nonlinear missile aerodynamic prediction method *MISDL* has been enhanced and applied to the prediction of the aerodynamic characteristics of missile and aircraft configurations employing trailing-edge flaps and ailerons for control. Various configurations have been investigated and compared with experimental data. These configurations include low aspect ratio missile fins and moderate aspect ratio fins/wings typical of missiles, fighters and combat UAVs. Speed regimes from subsonic through supersonic have been investigated. Nonlinear effects of body-shed and fin trailing vorticity and Mach number are included in the analysis. The use of flaps for the control of weapons systems and UAVs, as opposed to all movable control surfaces, has increased in recent years, and engineering-level methods are needed which can explicitly model and estimate performance for design and trade studies and to generate large databases for 6-DOF simulations.

Nomenclature

AR	=	aspect ratio (two fins joined at root)
C_l	=	rolling moment/$q_\infty S_R l_R$
C_m	=	pitching moment/ $q_\infty S_R l_R$; positive nose up
$C_{m\delta f}$	=	pitching moment derivative with flap deflection
C_N	=	normal force/ $q_\infty S_R$
C_{NF}	=	fin normal force/ $q_\infty S_R$
D	=	body diameter, maximum
L	=	body length
l_R,L_{REF}	=	reference length
q_∞	=	freestream dynamic pressure
S_R,S_{REF}	=	reference area
x_{CP}	=	fin chordwise center of pressure, or overall configuration axial center of pressure
y_{CP}	=	fin spanwise center of pressure
x_{HL}	=	fin hinge line loaction
x_{MC}	=	moment center
α	=	angle of attack, deg
δ	=	fin deflection angle
δ_F	=	flap deflection angle
λ	=	fin taper ratio
φ	=	roll angle, deg

I. Introduction

This paper discusses the enhancement and capability of the *MISDL* intermediate-level aerodynamics prediction methods to estimate the aerodynamic characteristics of flight vehicles with fins and wings employing trailing-edge flaps. The benefits of the nonlinear panel-based method include the capability for initial design, trade studies, and simulations. It is common when generating aerodynamic databases for initial 6-DOF simulations that the number of data points associated with flow conditions and control surface deflections exceeds 10,000. Flow conditions include Mach number, Reynolds number, angle of attack, and sidelip or roll angle, and control surface deflections include fin deflection angles and/or a variety of flap deflections. Computationally efficient methods to estimate aerodynamic are important. The *MISDL* method can analyze many flow conditions quickly to aid the engineer in the preliminary design

[1] Senior Research Engineer, 2700 Augustine Dr, Suite 200, Senior Member.

and conceptual stages to estimate loads for flight simulations and for structural analysis, and to prepare for more costly CFD runs and wind-tunnel tests. The *MISDL* code[1-4] is a panel-method-based prediction method enhanced to model missiles at high angles of attack including extensive vortex modeling. *MISDL* can model conventional as well as unconventional body shapes, fin planforms, and fins with arbitrary spanwise dihedral. The paneling method and has been enhanced to better model configurations employing flap control surfaces along any edge of the modeled lifting surfaces.

II. Technical Description

A. Description of *MISDL*

The intermediate-level aerodynamic prediction code *MISDL*[1-4] is based on panel methods and classical singularity methods enhanced with models for nonlinear vortical effects. It predicts longitudinal and lateral-directional aerodynamic characteristics including nonlinear Mach number and body and fin vortex wake effects. *MISDL* can model noncircular body configurations and configurations with unconventional fin shapes. The body of the missile is modeled with conformal mapping (if noncircular) and by either subsonic or supersonic sources/sinks and doublets for volume and angle of attack effects, respectively. The fin sections are modeled by a horseshoe-vortex panel method for subsonic flow and by constant pressure panels for supersonic flow. Up to three fin sections can be modeled, and nonlinear fin and body vortices are modeled. The body vorticity is modeled using the *VTXCHN* vortex-cloud method.[5,6] The overall calculation proceeds as follows: 1) the forebody loads are computed including effects of body vortex shedding and tracking, 2) loads within the forward fin set are calculated including the effects of forebody vorticity, 3) the vorticity shed from the forebody and the forward fin set is included as an initial condition in the *VTXCHN* module which tracks and models additional vortices shed from the afterbody, and 4) if second or third fin sets are present, steps 2 and 3 are repeated. A schematic of the calculation procedure and paneling layouts is shown in Fig. 1.

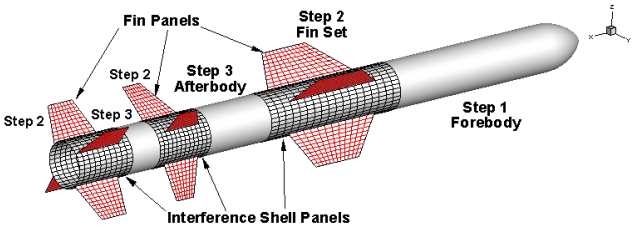

Figure 1. Calculation procedure and paneling layout.

Recent enhancements have included: additional options for specification of shed vortex properties (core size), improved modeling of deflected fin shed vorticity, better modeling of lifting surfaces with flaps, increasing the number of circumferential body panels within a fin section to better capture mutual fin-body carryover forces, and the option to extend the fin section body panels both forward and aft of the fin leading- and trailing-edges to better model the fin loading carryover.

The range of parameters of the *MISDL* code includes Mach numbers from 0.0 to 3.0 with a modified shock-expansion capability to higher supersonic speeds, angles of attack up to 20°, arbitrary roll angles, and rotational rate effects. For bodies alone, the angle of attack range limit exceeds 40°. Fins can have arbitrary planform shape and spanwise dihedral including modeling of wrap-around and folded fins.[4] An empirical stall model is included for modeling fins at high angles of attack. A version of *MISDL* employing an optimizer was used to design unconventional fin planforms for several design objectives including minimization of fin hinge moments and maximization of normal force.[5] Fig. 2 is an illustrative prediction for a circular ogive-cylinder body at high angle of attack. The predicted pressure distribution and body shed vortex wake are depicted. The body vortex shedding and tracking of individual vortices of the vortex "cloud" are colored in proportion to their individual strengths. The crossflow velocity vectors and the low pressure region below the vortices on the lee-side of the body show the strong influence of the body shed vorticity on both the local flow field and surface pressures.

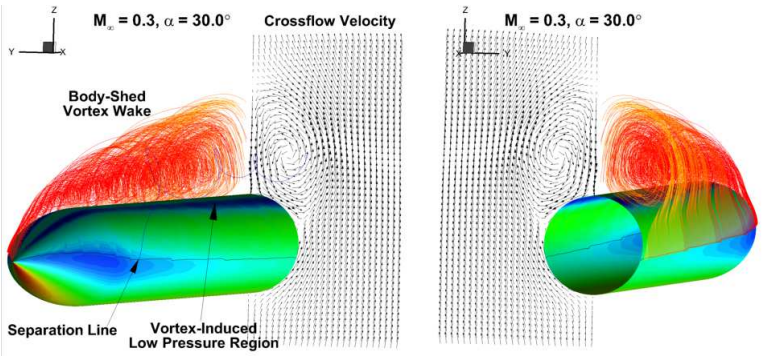

Figure 2. Example prediction of body-alone at high angle of attack.

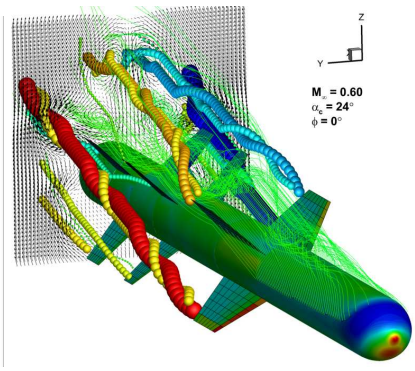

Figure 3. Three fin-set prediction.

Fig. 3 depicts predicted results for a three-fin section missile at high angle of attack. The predicted pressure coefficient is plotted on the body surface and the loading pressure, ΔC_P, is shown for the fins. Vortices are illustrated by symbols which are colored and sized in proportion to the vortex strength. The details of the flow fields predicted are useful for understanding the character of the flow at high angles of attack.

To model flaps in MISDL, input parameters are deflined which control the specification of flap geometries and panel distributions over the main fin and the flap panels. The deflection of the flaps is handled within the flow conditions input file making it easy to specify a rangle of deflections and to generate large aerodynamic databases for simulations and design. Fig. 4 illustrates the representation of a simple trailing-edge flap and a more complex wing with leading- and trailing-edge flaps, and outboard trailing edge ailerons. Currently, the flap modeling is for simple flaps; slotted and multiple segment flaps are not modeled explicitly.

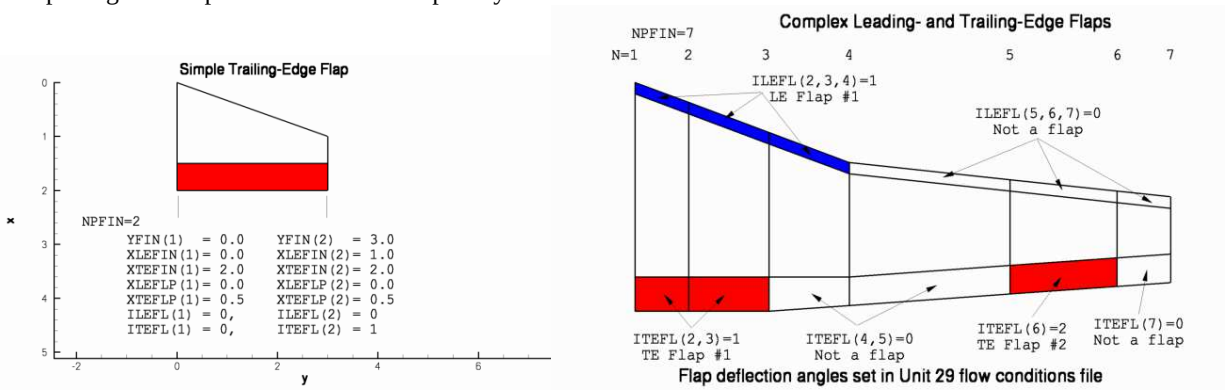

Figure 4. Modeling of a simple trailing-edge flap.

Within the methodology employed in the subsonic and supersonic panel methods, the panel deflections can be handled in two ways. The first incorporates the panel deflections as additional local camber within the boundary conditions formulated to solve for the panels strengths. The second method geometrically deflects the panels about the flap hinge line. The second option is a recent addition to the methodology and is currently under going additional testing. All results present in this paper utilize the "camber" option unless otherwise stated.

III. Results

This section presents longitudinal and lateral-directional aerodynamic predictions for several configurations employing flaps for control. These range from low to high aspect ratio fins/wings, and speeds from subsonic to supersonic.

NACA RM A53C20[7] – diamond-wing with full span flap

The body diamond-wing configuration shown in Fig. 5 was investigated. The wing aspect ratio is 2, and the chord length of the full span elevons is ¼ the local chord. The wing airfoil sections are NACA 63-0005. For the MISDL calculations, the body of Ref. 7 was approximated as an ogive-cylinder. Results are presented for a Mach number of 0.24.The low Mach number eliminates any compressibility effects. Results were obtained for flap deflections of -20, -15, -10, -5, 0, 5, and 20°. Fig. 6 compares measured and predicted lift and pitching moment characterstics utilizing the recommended input values for the wing including empirical values for the conversion of "suction forces" to normal force using the Polhamus suction analogy,[8] and for the empirical wing stall model.

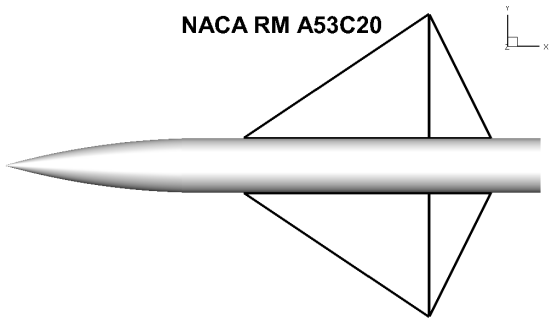

Figure 5. NACA RM A53C20 diamond wing/flap.

The predicted results in Fig. 6 agree well with the experiment for angles on attack below 10° and for flap deflection up to 10°. For zero flap deflection, the MISDL prediction, with default settings for its empirical stall model, has the lift curve slope reducing above 12° angle of attack.

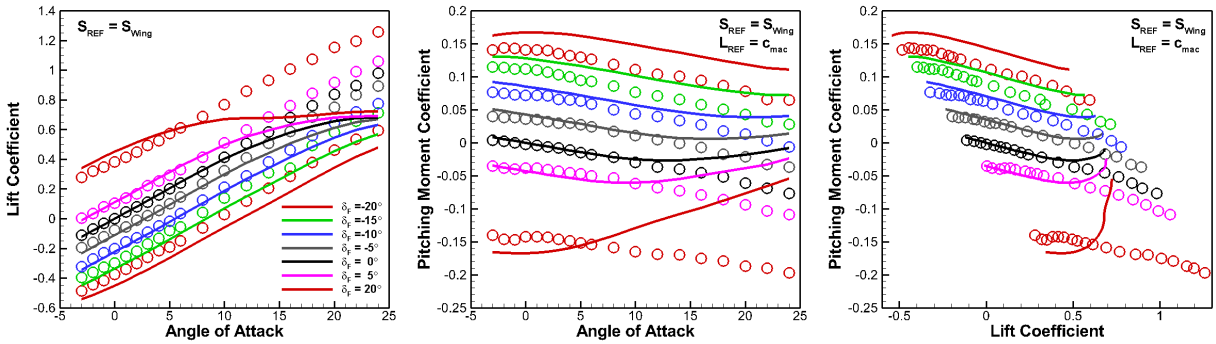

Figure 6. MISDL prediction using standard wing stall model.

Because the results indicate that MISDL is predicting an early stall for this diamond wing, the section stall model's maximum lift, $C_{\ell_{max}}$, was increased by adjusting a user input variable to better match the experiment. In addition, flaps increase the maximum lift coefficient that is achieved by the airfoil section of the wing. The comparsions in Fig. 7 indicate much better agreement at the higher angles.

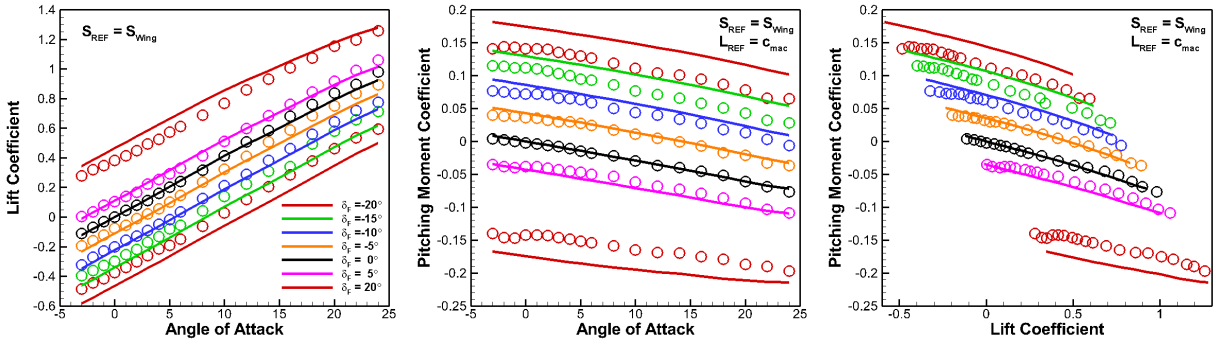

Figure 7. Prediction with increased maximum section lift.

The largest differences between the measured and predicted results occur at the largest flap deflection angles. This is expected due to the potential for flow separation and lower loads. MISDL is a potential method and is not capable of explicitly predicting effects of flow separation caused by large flap deflections. For large flap deflection angles, USAF DATCOM[9] (Fig. 4.1.1-40) contains an empirical factor, K' or F_δ, used to adjust the flap deflection angle. Blake and Burns[10] utilized the methodology of USAF DATCOM when adding a trailing-edge flap modeling capability to Missile DATCOM. The F_δ factor is a function of the flap deflection angle and the ratio of the flap chord to the airfoil chord: $F_\delta = f(c_f/c, \delta_F)$. Results utilizing an effective flap deflection angle based on the correction factor of Fig. 4.1.1.1-40 of Ref. 9 are shown in Fig. 8. Only the 15 and 20° flap deflection conditions are affected. For $\delta_F = 20°$ the correction results in an effective flap deflection of 17° ($F_\delta = 0.85$), which brings both the +20 and -20° deflection result into agreement with the experiment. For $\delta_F = 15°$, the correction is smaller and less improvement is seen.

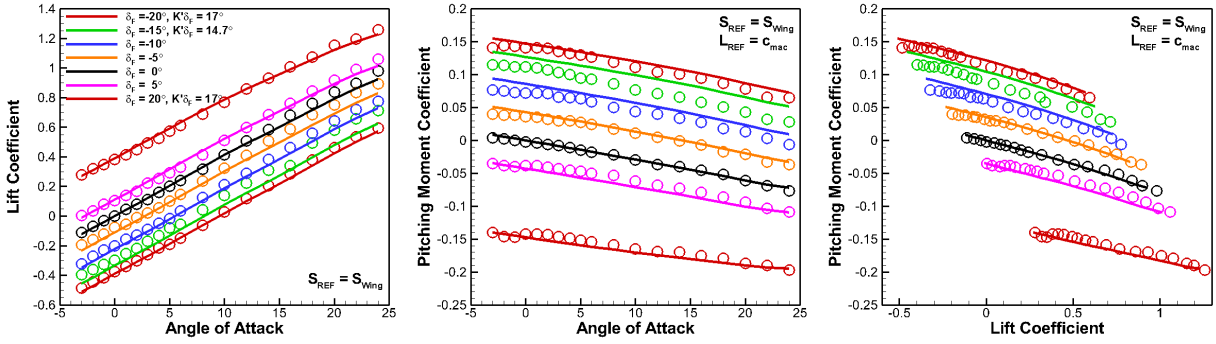

Figure 8. Prediction including empirical correction for large flap deflection angle.

NACA RM A52D01c[11] - delta wing with full-span constant-percent-chord flap

The body delta-wing configuration shown in Fig. 9 was investigated. The wing aspect ratio is 2 with a leading-edge sweep of 63°. The chord length of the full span flap is ¼ of the local chord. The wing airfoil sections are NACA 63-0005. For the MISDL calculations, the body was approximated as an ogive-cylinder. The flap effectiveness is presented as a function of Mach number and flap deflection angle in Fig. 10. Because the flap deflection is modeled through equivalent camber, the deflection angle must be input in the streamwise/chordwise direction rather than as a rotation about a swept hinge line indicated in Fig. 9. The streamwise flap deflection is given by:

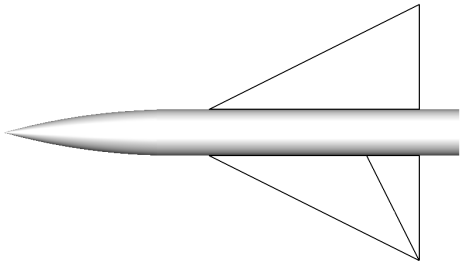

Figure 9. NACA RM A52D01c delta wing/flap.

$$\delta_F = \tan^{-1}(\tan\delta_{HL}\cos\Lambda_{HL})$$

In addition, for subsonic Mach numbers and $\delta_F > 10°$, the F_δ correction of USAF DATCOM[9] (Fig. 4.1.1-40) is applied as described above.

Flap effectiveness results at $\alpha = 0°$ were obtained for δ_F corresponding to δ_{HL} angles of +5, 0, -2.5, -5, -10, -15, -20, and -25°. The flap effectiveness at supersonic speeds is predicted very well. At subsonic speeds, the effectiveness is estimated well up to 10° flap deflection. Above 10°flap deflection, and for the transonic Mach numbers of 0.8 and 0.9, the predictions overestimate the effectiveness of the flap. This is seen in the lift coefficient. For $M_\infty = 0.6$, the predictions are in agreement with the experiment for deflections of -15 and -20 but have the wrong trend with increasing Mach number. Deflection of flaps at transonic speeds often results in shocks on the suction surface as the flow accelerates. These effects require additional investigation.

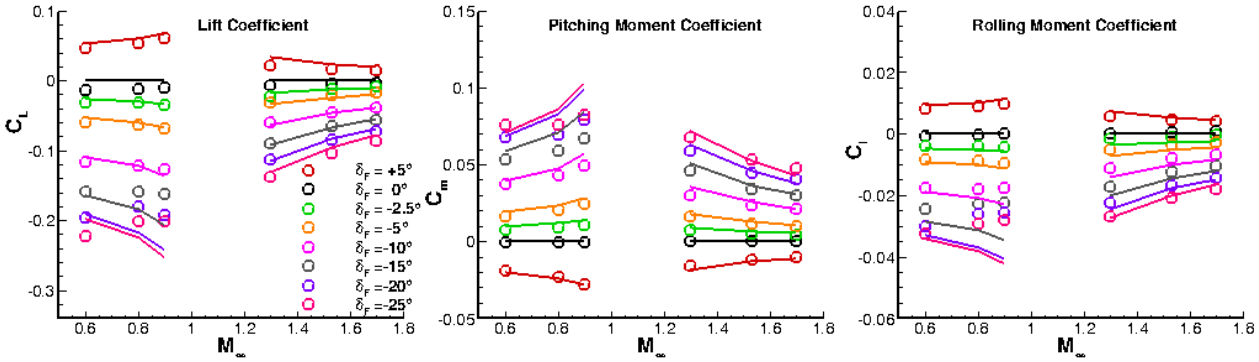

Figure 10. Delta wing full-span constant-percent-chord flap effectiveness.

NASA TM X-2367[12] – low aspect ratio fin at supersonic speeds

The body-fin configurations of NASA TM X-2367 is shown in Fig. 11. The body consists of a 2.67 caliber blunted-cone-ogive nose combination followed by a six-caliber cylinder. The fin has a root chord of 4.33 calibers, an exposed span of 1.33 calibers, and a leading edge sweep of 72.9 degs. The fin aspect ratio (two fins joined at the root) is 1.23. The flap chord is 7.7% of the root chord and extends from the body a length of one diameter. Figs. 12 and 13 show overall normal force and pitching moment coefficients for Mach 1.50 and 1.90, respectively. Results are shown for the body alone and the body-fin combination with 0.0 and -20 deg. deflection of the flaps. In general, the predicted and measured results are in good agreement for low and moderate angles of attack. The measured and predicted flap effectiveness derivative at zero degrees angle of atttack for Mach numbers from 1.50 to 4.63 are plotted in Fig. 14.

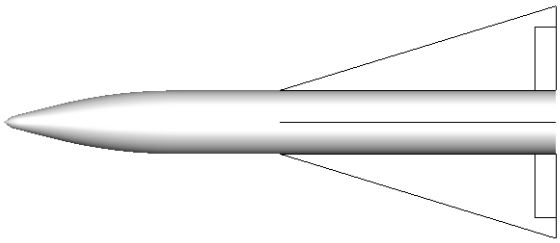

Figure 11. Body-wing, NASA TM X-2367.

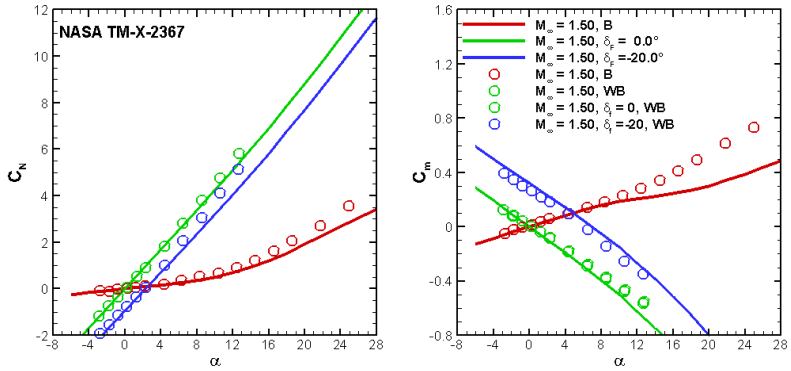

Figure 12. Mach = 1.50

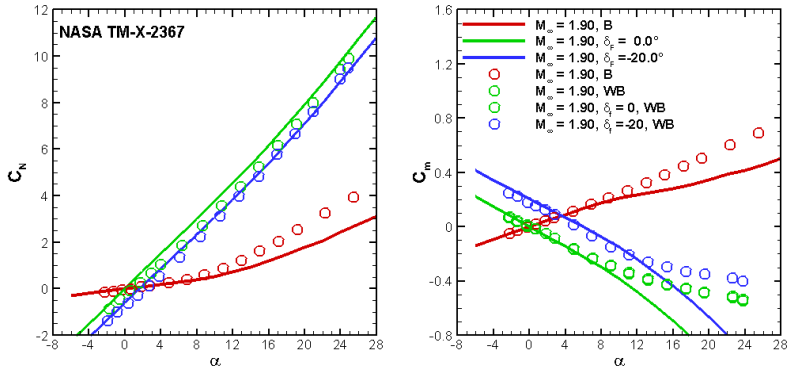

Figure 13. Mach = 1.90

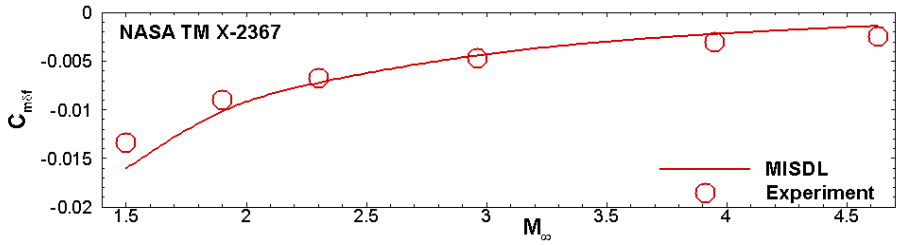

Figure 14 Flap deflection effectiveness derivative, per deg.

Tailless Fighter, AIAA 93-4000[13] and WL-TR-92-3111[14]

Some results presented in AIAA 93-4000[13] for the subsonic tailless fighter configuration of WL-TR-92-311[14] have been investigated with the *MISDL* code. This configuration was tested with trailing-edge flaps and with all-movable wing tips. Fig. 15 depicts the configuration with all-movable tips modeled with geometric deflections in *MISDL*. Fig. 16 compares measured and predicted results for three roll control deflections left/right: +15/-15, 0/-30, and -15/-45. The *MISDL* estimates are based on the standard *MISDL* model with the empirical wing sectional lift stall model. Because the wing tip control surfaces are not analogsis to trailing-edge flaps, no additional deflection effectiveness parameters are used. The preliminary results in Fig. 16 indicates that the *MISDL* model estimates the +15/-15 roll control geometrically deflected the wing tips. The trend of the 0/-30 and -15/-45 controls is predicted, but the

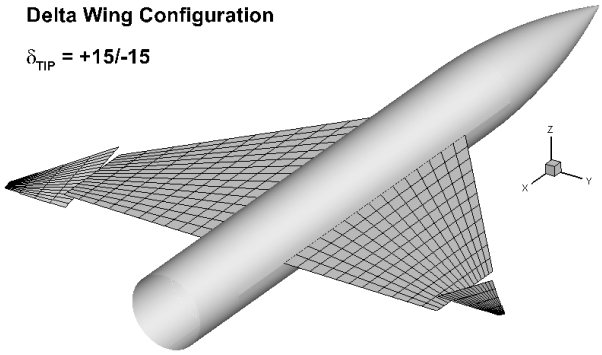

Figure 15. Tailless fighter with movable wing tips.

maximum roll is higher and at a larger angle of attack. These are very large deflection angles, and therefore, the results depend on the empirical sectional lift stall model in *MISDL*. This stall model was developed for correcting airfoil lift curve properties for wings, but may not be fully applicable to configuations such as the all-movable wing tips where gap effects and flow separation have strong influences. Capturing some of the trends is encouraging. To better understand the rolling moment characteristics, Fig. 17 plots the normal forces on the right and left wings of the configuration. The red curve corresponds to zero wing tip deflection. The predicted rolling moment characteristics shown in Fig. 16 are the result of differences in the forces on left and right wings with the primary differences in loading acting on the deflected tips. The three deflection sets in Fig. 17 correspond to the three curves in Fig. 16. The middle curve of Fig. 17 depicts δ_{TIP} = 0/-30 results and correspond to the green curve in Fig. 16. The characteristics of the rolling moment arise from subtle differences in the wing loadings. For +15/-15 deflections, both wings are completely stalled at the highest angle of attack resulting in a near zero rolling moment. To further illustrate the wing loading and resulting rolling moment, Fig. 18 show the span load distribution for three flow conditions: 1) α = 15°, δ_{TIP} = 0/0; 2) α = 0°, δ_{TIP} = +15/-15, and 3) α = 15°, δ_{TIP} = +15/-15. The α = 15°, δ_{TIP} = 0/0 configuration does not produce a net rolling moment and is used a a reference for the α = 15°, δ_{TIP} = +15/-15. For both of these conditions, the stall model is engaged. The -15° deflection on the right wing unloads the tip and this effect carries over to the inboard wing. The left wing at +15° indicates that the wing tip is stalled; the loading is nearly the same as the undeflected wing result. And, the α = 0°, δ_{TIP} = +15/-15 results show the characteristics of the span load distribution which includes only the tip deflection effect.

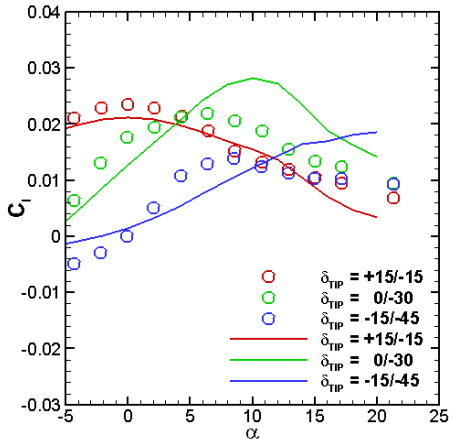

Figure 16. All movable wing-tip roll control.

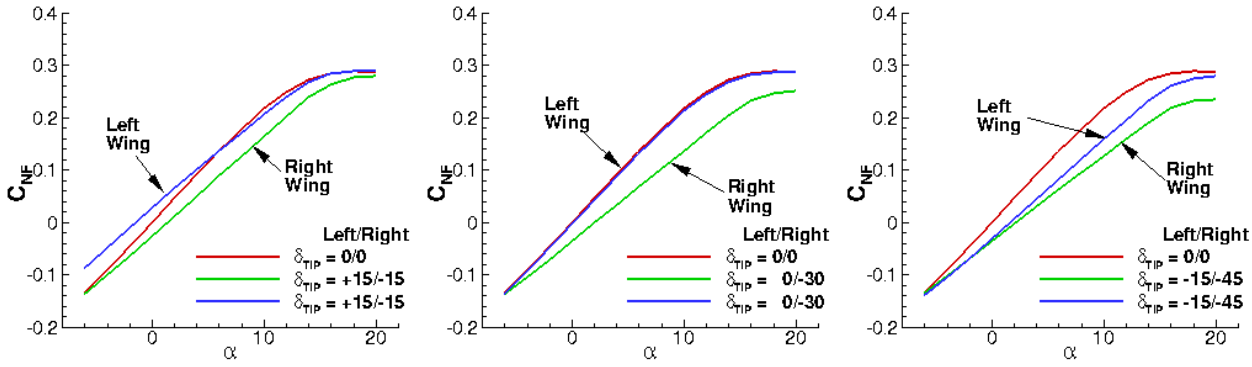

Figure 17. Predicted right and left wing normal force with deflected tips.

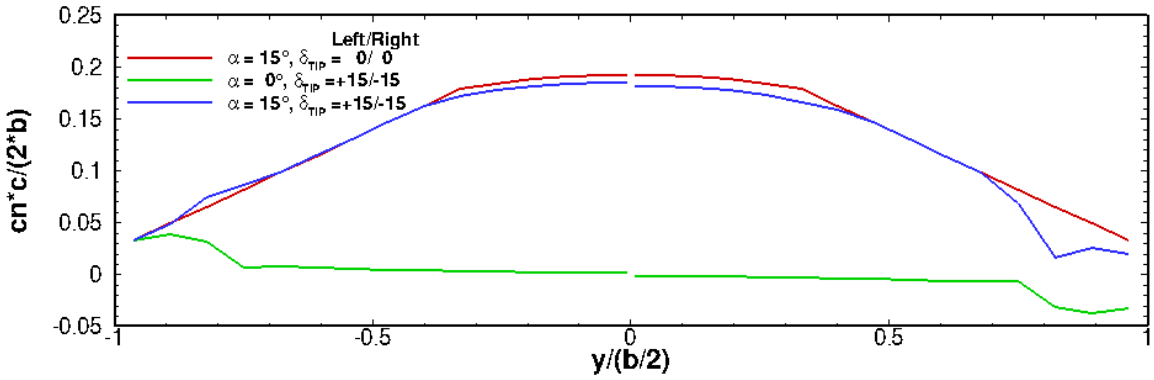

Figure 18. Predicted span load distributions for delta wing with all-movable wing tips.

IV. Conclusion

MISDL is an engineering method suitable for creating large aeroynamic databases for conceptual and preliminary design. This paper presents an initial investigation of the ability of the prediction code to estimate the aerodynamics of configuration employing trailing-edge flaps for control. The methodology employed predicts flap effectiveness for preliminary design and analysis efficiently. The current study indicated that the *MISDL* flap modeling benefits from empirical correction factors for flap deflection above 10°. The correlation factor in USAF DATCOM provides a means for this and will be include in the methodology. In addition, high-fidelity results from wind tunnel tests and/or CFD, at specific flow conditions, can be used to develop corrections to *MISDL* generated databases through data fusion methods. Modeling of geometrically deflected flaps, rather than through the camber distribution, is also being investigated. Fundamentally, the geometric deflection is preferred, but practically, issues arise in the panel solution due to panel-on-panel influences, especially for panels next to the body. In addition, future work will investigate individual flap forces and hinge moments about the flap hinge line.

References

[1]Lesieutre, D. J., Love, J. F., and Dillenius, M. F. E., "Prediction of the Nonlinear Aerodynamic Characteristics of Tandem-Control and Rolling-Tail Missiles," AIAA 2002-4511, Aug. 2002.

[2]Dillenius, M. F. E., Lesieutre, D. J., Hegedus, M. C., Perkins, S. C., Jr., Love, J. F., and Lesieutre, T. O., "Engineering-, Intermediate- and High-Level Aerodynamic Prediction Methods and Applications," *Journal of Spacecraft and Rockets*, Vol. 36, No. 5, Sep.-Oct. 1999, pp. 609-620.

[3]Lesieutre, D. J., Dillenius, M. F. E., and Gjestvang, J., "Application of MISDL/KDA Aerodynamics Prediction Method to Penguin Missile," AIAA 2002-0277, Jan. 2002.

[4]Lesieutre, D. J., Dillenius, M. F. E., and Lesieutre, T. O, "Multidisciplinary Design Optimization of Missile Configurations and Fin Planforms for Improved Performance," AIAA 98-4890, Sep. 1998.

[5]Hegedus, M. C., Dillenius, M. F. E., Perkins, S. C., Jr., and Mendenhall, M. R., "Improved Version of the VTXCHN Code," NEAR TR 498, Nielsen Engineering & Research, Mountain View, CA, Aug. 1995.

[6]Mendenhall, M. R., Perkins, S. C., Jr., and Lesieutre, D. J., "Vortex Cloud Model for Body Vortex Shedding and Tracking," *Tactical Missile Aerodynamics: Prediction Methodology*, ed. by M. R. Mendenhall, AIAA, 1992, pp. 225-285.

[7]Smith, D. W. and Reed, V. D., "Subsonic Static Longitudinal Stability and Control Characteristics of a Wing-Body Combination Having a Pointed Wing of Aspect Ration 2 With Constant-Percent-Chord Trailing-Edge Elevons," NACA RM A53C20, May 1953.

[8]Polhamus, E. C., "Prediction of Vortex-Lift Characteristics Based on a Leading-Edge Suction Analogy," Jornal of Aircraft, Vol. 8, Apr. 1971, pp. 193-199.

[9]Hoak, D. E., et al, "USAF Stability and Control DATCOM," AFWAL TR-83-3048, Oct. 1960 (revised 1978).

[10]Blake, W. B. and Burns, K. A., "Missile Datcom: Recent Enhancements Including Trailing Edge Flap Effects," AIAA 1994-0027, Jan. 1994.

[11]Boyd, J. W., "Aerodynamic Characteristics of Two 25-Precent-Area Trailing-Edge Flaps on an Aspect Ratio 2 Triangular Wing at Subsonic and Supersonic Speeds, NACA RM A52D01c, July 1952.

[12]Trescot, Jr., C. D., "Longitudinal Aerodynamic Characteristics at Mach 1.50 to 4.63 of a Missile Model Emploting Various Canards and a Trailing-Edge Flap," NASA TM X-2367, Oct. 1971.

[13]Simon, J. M., Blake, W. B., and Multhopp, D., "Control Concepts For A Vertical Tailless Fighter," AIAA 1993-4000, 1993.

[14]Baldwin, A. W. and Adamczak, D. W., "Analysis of Experimental Aerodynamic Control Devices for Control of Tailless Fighter Aircraft," WL TR-92-3111, Nov. 1992.